

AD-A042 254

MINNESOTA UNIV MINNEAPOLIS PHYSICAL ELECTRONICS LAB
PHOTOCATHODE STUDY TO REDUCE NOISE.(U)
MAY 77 W T PERIA

F/G 9/1

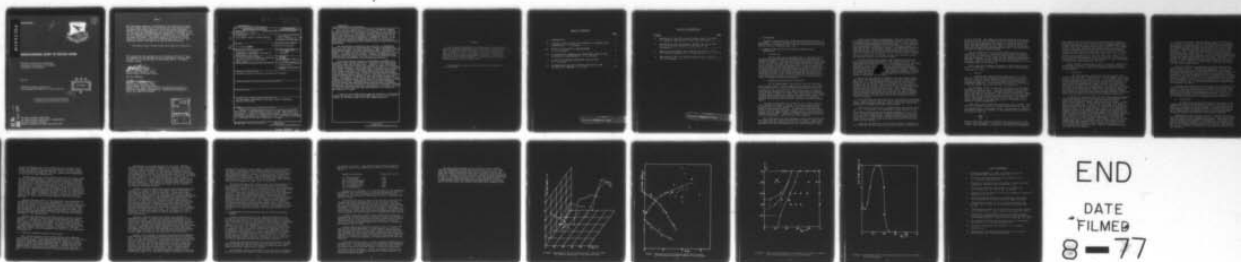
UNCLASSIFIED

AFAL-TR-76-38

F33615-72-C-2105
NL

| OF |

ADA042254



END

DATE
FILMED
8-77

AD A 042254

AFAL-TR-76-38



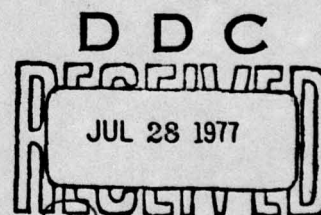
10

PHOTOCATHODE STUDY TO REDUCE NOISE

PHYSICAL ELECTRONICS LABORATORY
ELECTRICAL ENGINEERING DEPARTMENT
UNIVERSITY OF MINNESOTA

MAY 1977

TECHNICAL REPORT AFAL-TR-76-38
FINAL REPORT FOR PERIOD JULY 1972 thru MAY 1975



E

Approved for public release; distribution unlimited

AD No. _____
DDC FILE COPY

AIR FORCE AVIONICS LABORATORY
AIR FORCE WRIGHT AERONAUTICAL LABORATORIES
AIR FORCE SYSTEMS COMMAND
WRIGHT-PATTERSON AIR FORCE BASE, OHIO 45433

NOTICE


When Government drawings, specifications, or other data are used for any purpose other than in connection with a definitely related Government procurement operation, the United States Government thereby incurs no responsibility nor any obligation whatsoever; and the fact that the Government may have formulated, furnished, or in any way supplied the said drawings, specifications, or other data, is not to be regarded by implication or otherwise as in any manner licensing the holder or any other person or corporation, or conveying any rights or permission to manufacture, use, or sell any patented invention that may in any way be related thereto.

This technical report has been reviewed and is approved for publication.

This report has been reviewed by the Information Office (OI) and is releasable to the National Technical Information Service (NTIS). At NTIS, it will be available to the general public, including foreign nations.


CLYDE L. WOODARD, Chief
Electro-Optic Detectors Group
Electro-Optics Technology Branch

FOR THE COMMANDER


WILLIAM C. SCHOONOVER, Chief
Electro-Optic Detectors Group
Electro-Optics Technology Branch

Copies of this report should not be returned unless return is required by security considerations, contractual obligations, or notice on a specific document.

ATR FORCE - 8 JUN 77 - 100

ACCESSION for	
NTIS	White Section <input checked="" type="checkbox"/>
DDC	Buff Section <input type="checkbox"/>
UNANNOUNCED	<input type="checkbox"/>
JUSTIFICATION	
BY	
DISTRIBUTION/AVAILABILITY CODES	
Dist. AVAIL. and/or SPECIAL	
A	

⑨ Final rept. 1 Jul 72 -
31 May 75,

UNCLASSIFIED

SECURITY CLASSIFICATION OF THIS PAGE (When Data Entered)

REPORT DOCUMENTATION PAGE		READ INSTRUCTIONS BEFORE COMPLETING FORM
1. REPORT NUMBER ①8 AFAL-TR-76-38 ①9	2. GOVT ACCESSION NO.	3. RECIPIENT'S CATALOG NUMBER
4. TITLE (and Subtitle) ⑥ Photocathode Study to Reduce Noise.	5. TYPE OF REPORT & PERIOD COVERED Final Report July 1, 1972-May 31, 1975	
7. AUTHOR(s) ⑩ W. T. Peria	6. PERFORMING ORG. REPORT NUMBER	
9. PERFORMING ORGANIZATION NAME AND ADDRESS University of Minnesota Department of Electrical Engineering Minneapolis, MN 55455	8. CONTRACT OR GRANT NUMBER(s) ①5 F33615-72-C-2105	
11. CONTROLLING OFFICE NAME AND ADDRESS Air Force Avionics Laboratory, AFAL/DHO Wright Patterson Air Force Base Ohio 45433	10. PROGRAM ELEMENT, PROJECT, TASK AREA & WORK UNIT NUMBERS ①6 2001-03-31 68204 F	
14. MONITORING AGENCY NAME & ADDRESS (if different from Controlling Office)	12. REPORT DATE ①1 May 77	
	13. NUMBER OF PAGES 22-12 24p.	
	15. SECURITY CLASS. (of this report) Unclassified	
	15a. DECLASSIFICATION/DOWNGRADING SCHEDULE	
16. DISTRIBUTION STATEMENT (of this Report) Approved for public release; distribution unlimited.		
17. DISTRIBUTION STATEMENT (of the abstract entered in Block 20, if different from Report)		
18. SUPPLEMENTARY NOTES		
19. KEY WORDS (Continue on reverse side if necessary and identify by block number) Photocathodes, Semiconductor Surfaces, Alkali Antimonides, Electron Scattering		
20. ABSTRACT (Continue on reverse side if necessary and identify by block number) Energy loss spectroscopy was used in a study of the Ge(100)- Cs-O system. A characteristic loss at 3 eV was identified and is ascribed to a transition between surface bands. The results are interpreted in terms of a model which requires different overlayer structures (depending upon composition) and a work function minimum at 1 monolayer of Cs and 1/2 monolayer of oxygen. → OVER		

DD FORM 1 JAN 73 1473

EDITION OF 1 NOV 65 IS OBSOLETE

UNCLASSIFIED

SECURITY CLASSIFICATION OF THIS PAGE (When Data Entered)

233 630 113

Contd
UNCLASSIFIED

SECURITY CLASSIFICATION OF THIS PAGE(When Data Entered)

More than 15 years after its discovery, $\text{Na}_2\text{KSb}(\text{Cs})$ remains an important photocathode material, but control of its formation remains a problem. In the present studies Auger electron spectroscopy (AES) was used to determine the atomic species present in the surface region during formation of $\text{Na}_2\text{KSb}(\text{Cs})$ films. It was found that the electron bombardment incidental to the use of the AES technique could cause sample changes, but this problem was eliminated for samples that were heated during or after constituent depositions.

The $\text{Ge}(100)/\text{Cs}/\text{O}$ photosurface and surfaces at intermediate stages of activation are characterized in terms of photoemission work function, Auger electron spectroscopy (AES), low energy electron diffraction (LEED), and elastic specular electron reflectivity (ESER). An electrical and structural model is proposed for $\text{Ge}/\text{Cs}/\text{O}$ which is consistent with this data. A number of experiments are reported which investigate the sensitivity of the $\text{Ge}/\text{Cs}/\text{O}$ surface to deviations from chemical and structural perfection.

Low energy electron scattering measurements were made on an atomically clean $\text{Ge}(100)$ surface as a function of primary energy, scattering angle and surface order. Analysis of the elastically diffracted electrons indicated the probable existence of a $\text{Ge}(100) 4 \times 2$ surface structure. With appropriate inner potential corrections, most elastic intensity maxima were found to satisfy either kinematical Bragg conditions or secondary Bragg conditions associated with maxima of another beam. Inelastic electron energy distributions displayed numerous characteristic loss peaks due to interband electron excitation in addition to bulk and surface plasmon loss peaks. Measurements of the energy and angular distributions of the inelastic electrons showed the existence of strong inelastic electron diffraction effects. Measurements of the low energy secondary electron energy distributions produced observations of secondary peaks which could be attributed to diffraction of secondary electrons. In addition, secondary peaks were observed which are felt to be due to direct electron emission from local maxima in the conduction band density of states.

A study of the $\text{Si}(100)\text{-Cs-F}$ system was carried out to determine whether CsF would be a more stable NEA coating for Si and also as a check on the Levine model of Cs and oxygen adsorption.

UNCLASSIFIED

SECURITY CLASSIFICATION OF THIS PAGE(When Data Entered)

PREFACE

The research described in this report was carried out in the Physical Electronics Laboratory of the University of Minnesota under Contract No. F33615-72-C-2105 - Project No. 2001, Task 03, Work Unit 31, between July 1, 1972 and May 31, 1975. The work was supervised by W. T. Peria, Professor of Electrical Engineering, University of Minnesota, Minneapolis, Minnesota. The project monitor is W. H. Nelson, AFAL/DHO, Air Force Avionics Laboratory, Wright-Patterson Air Force Base, Ohio.

This technical report has been reviewed and is approved for publication.

TABLE OF CONTENTS

	<u>Page</u>
I. INTRODUCTION	1
II. A STUDY OF THE Ge(100)-Cs-O SURFACE BY ELECTRON LOSS SPECTROSCOPY - Y. Viswanath	1
III. STUDIES OF Na ₂ KSb(Cs) PHOTOCATHODES - P. A. Lindfors	6
IV. AN ELECTRICAL, CHEMICAL AND STRUCTURAL STUDY OF THE Ge(100)-Cs-O PHOTOCATHODE - R. E. Ericson	7
V. A STUDY OF ELECTRON SCATTERING FROM Ge(100) - R. L. Erickson	8
VI. PHOTOELECTRIC AND WORK FUNCTION STUDIES OF THE Si(100)-Cs-F SURFACE - F. J. Kub	10

PRECEDING PAGE, BLANK, NOT FILMED

LIST OF ILLUSTRATIONS

<u>Figure</u>	<u>Page</u>
1. Magnitude of the 3eV electron energy loss of Ge(100) vs. chemical composition of the Cs-O overlayer.....	13
2. Magnitude of the 3eV electron energy loss on Ge(100) vs. the effective dielectric constant of the overlayer.....	14
3. Phase diagram showing the composition ranges in which the various branches of Fig. 2 are valid.....	15
4. Magnitude of the 3eV electron energy loss on Ge(100) vs. Cs coverage.....	16

PRECEDING PAGE, BLANK, NOT FILMED

I. INTRODUCTION

Complete reports have been issued on several of the topics of this report. For those cases only the main conclusions will be reproduced here. The work of Sec. II has not previously been reported and will be more thoroughly described.

II. A STUDY OF THE $\text{Ge}(100)\text{-Cs-O}$ SURFACE BY ELECTRON LOSS SPECTROSCOPY.

1. Introduction

Several years ago we suggested (ref. 1) the possibility of detecting surface states on semiconductors by examining the energy distribution of low energy electrons backscattered from the crystal in question. The idea was that characteristic energy losses of the incident electrons could occur when they excited electrons from a filled to an unfilled surface state. A special apparatus was constructed and has been described in a previous report (ref. 2). It was used mainly for a detailed structural study of $\text{Ge}(100)$ but an energy loss feature was detected which seemed to be worth investigating further. This report describes the additional work which has been carried out in order to identify the origin of the loss feature and to utilize it in furthering the understanding of alkali and oxygen-covered semiconductors.

2. Apparatus and Experimental Technique

All the measurements were carried out in an Ultek UHV metal belljar system. Initial pumping from atmosphere to 10^{-3} Torr was accomplished by liquid N_2 cooled zeolite sorption pumps and pressures of less than 10^{-10} Torr were attained with the help of 100 liter/sec titanium getter-ion pumps (with auxiliary titanium getters) after a bakeout to $\sim 280^\circ\text{C}$. The capabilities of the system included work function and photoemission measurements, LEED, Auger Electron Spectroscopy (AES), sputter cleaning, ion deposition, Specular Electron Reflectivity (SER) and Energy Loss Spectroscopy (ELS).

The sample manipulator was capable of 2.5" vertical motion, $\sim 360^\circ$ rotation and could be tilted. The tantalum sample holder was mounted on a ceramic insulator so that the target could be biased at any desired potential. It contained an internal heater filament (used to heat the sample holder) and a target which is in contact with the sample holder. Temperatures up to 650°C could be obtained by this means. Additional target heating was provided by electron bombardment. The target was .707 cm square.

The vacuum system was also equipped to admit spectrographically pure gases through Granville-Phillips type C valves. Argon, used for sputtering, was further purified by a cataphoretic procedure. Helmholtz coils were provided to null the earth's magnetic field.

LEED and Auger Electron Spectroscopy (AES) measurements were carried out using a four-grid hemispherical system. An ac modulation-phase-sensitive detection method was used for energy analysis of the electrons backscattered from the surface. In the Auger mode the second harmonic component of the total collector current is displayed against the retarding voltage. The LEED-Augur system was also used for ELS. The primary energy was typically ~100 eV and losses which were ≤ 40 eV from the elastic peak were monitored. To more easily detect the features in ELS, the third harmonic component (which is proportional to d^2N/dE^2) of the total collector current was displayed against the retarding voltage.

Specular Electron Reflectivity (SER) measurements were made using a slightly modified version of the Zollweg gun (ref. 3). This method has several advantages: the specular, elastic reflection coefficient (i.e. the intensity of the (00) LEED beam) can be measured at normal incidence, using an essentially monochromatic electron beam ($\Delta E \sim 0.05$ eV). The same gun can be used to measure work function changes by the retarding potential method. A plot of the target current vs. target-cathode potential difference is made; shifts of these curves along the voltage axis give directly the change in the target work function.

The Cs ion gun employed a thermally activated cesium source. The design, construction and operation of the gun is described by Weber (ref. 4). The advantage of the ion gun was the ability to determine the Cs coverage simply by measuring the total charge incident upon the crystal. This can be done if the neutral atom output of the gun is negligible and if the ion sticking coefficient is unity over the entire coverage range. Weber measured the neutral and impurity emission to be about ~2.5%. The assumption that the sticking coefficient was unity over the entire coverage range also seems justified since the Cs Auger signal was found to be proportional to the deposited charge over the whole coverage range of interest.

Oxygen pressure was monitored using a Bayard-Alpert ionization gauge. Oxygen coverages were obtained by calibrating the oxygen AES signal versus exposure (pressure x time), taking into account the variation of sticking coefficient with coverage.

The sputtering gun was of a standard design described by Riach (ref. 5). It provided an ion bombardment current density of 40-50 $\mu\text{A}/\text{cm}^2$ at 50-200 eV energy for Argon pressures of $1 - 2 \times 10^{-3}$ Torr. Sputtered surfaces were annealed by heating at ~650°C for 30 minutes and cooling slowly. Annealed surfaces always yielded very good (2×1) LEED patterns and SER spectra characteristic of clean, ordered surfaces (SER is extremely sensitive to long range order over the surface).

A typical run consisted of cleaning the sample, characterizing it by AES, SER and ELS, observing the LEED patterns and measuring

the work function. The sample was then positioned in front of the Cs ion gun and the desired amount of Cs was deposited in predetermined steps until saturation was achieved. At each step all the above mentioned measurements were made. A controlled amount of oxygen was then admitted into the system to adsorb on the surface. Again the aforementioned measurements were made. The sequence was repeated for varying oxygen coverages.

Another sequence of runs involved depositing known varying amounts of Cs initially on the clean Ge(100) surface and exposing the surface to oxygen until oxygen did not adsorb any longer for moderate exposures. At each stage the above mentioned measurements were made. Experiments were repeated with varying known amounts of oxygen initially present on the surface and depositing Cs in predetermined steps until saturation.

After each run the sample was heated to $\sim 650^\circ\text{C}$ electron bombarded, and annealed. The total pressure in the system was always less than 10^{-10} Torr.

3. Results

A typical ELS spectrum showed peaks near 3, 5, 9 and 16.5 eV. The 16.5 and 9 eV peaks are identified with the excitation of bulk and surface plasmons, respectively, while the remaining two peaks (3 and 5 eV) are thought to indicate surface interband transitions. The following discussion will focus mainly on the two plasmon excitations and the 3 eV transition.

The magnitude of the 3 eV peak as a function of Cs and oxygen coverages is shown in Fig. 1. The data was obtained for the case where Cs was adsorbed first. Reversing the order of adsorption had no influence on the results. The electron reflectivity, however, showed that the most prominent feature (related to long range surface order) was an order of magnitude larger when Cs was adsorbed first. This seems to indicate that the 3 eV transition is not strongly dependent on the long range order of the surface but is primarily a localized phenomenon.

Each time a loss spectrum was measured it was, of course, also possible to measure the bulk and surface plasmon energies (E_{bp} and E_{sp} , respectively). From these values it was possible to calculate an effective dielectric constant of the adsorbed layer according to the relation (ref. 6).

$$\epsilon = \left(\frac{E_{bp}}{E_{sp}} \right)^2 - 1$$

Figure 2 shows the correlation between the magnitude of the 3 eV loss and the calculated ϵ . In spite of the large apparent scatter, it does seem reasonable to regard the relationship as 3-branched.

This would not be very interesting and the significance would be quite unclear were it not for the fact that it appears possible to correlate each branch with a certain range of surface layer composition. This fact is demonstrated on Fig. 3 where all of the points of Fig. 2 have been placed on a cesium-oxygen phase diagram and identified according to the branch of Fig. 2 from which they originated. Figure 3 seems to imply that curve II of Fig. 2 is associated with the composition region near Cs_2O while curve I is for compositions somewhat more Cs rich than the latter. Region IV of Fig. 3 denotes the composition regime in which the 3 eV loss is not observed at all, while region III and curve III of Fig. 2 correspond to compositions more oxygen-rich than Cs_2O .

Figure 4 shows the magnitude of the 3 eV loss as a function of Cs coverage (no oxygen). We focus attention on this particular curve because data is available from other experiments, to which it can be compared.

4. Discussion

The most important issue to be resolved is that of the origin of the 3 eV loss. Since it exists in the absence of an overlayer and its magnitude is so sensitive to the overlayer composition, it seems necessary to associate it with the germanium surface. The drastic magnitude changes can then most readily be interpreted as resulting from correspondingly drastic changes in the density of final states available for the transition. The transition itself must then occur from states approximately 3 eV below the Fermi level to states at the Fermi level. Small adsorption-related changes in the location of the Fermi level relative to the electronic energy level structure would then cause large occupancy changes in the final states and thus modify the intensity of the observed transition.

If the energy range over which the final states extend is small, (likely, because, as we have seen, they seem to be localized) then Fermi level changes required to cause the observed effects could be small enough to escape detection by direct means. In fact, Mularie and Jeanes (ref. 7) have sought such Fermi level changes due to cesium adsorption of Ge(100) and found them to be below the detection level. On the other hand, in a study of Na adsorption on Ge(111), Riach (ref. 8) found the Fermi level to move towards the conduction band at low coverages, back towards the valence band at somewhat higher coverages and finally towards the conduction band again as saturation coverage was approached. If we assume that Fermi level changes of the same sense (though of much lower magnitude) are occurring as a result of cesium adsorption on Ge(100), the trends in Fig. 4 can be explained. For example, if in the coverage range beyond about 0.3, the Fermi level is moving away from the valence band edge (analogy with Ge(111)-Na), more and more of the final states become occupied until finally the intensity of the 3 eV transition is reduced to zero. Similar considerations apply for other coverage regions.

The conclusion that a band of surface states exists at the Fermi level (and thus near the valence band edge) is in agreement with the work of Shepherd (ref. 9). He found from field emission measurements a band of surface states centered about 0.2 eV above the valence band edge and about 0.2 eV wide (full width at half maximum). A band of this width would seem to permit more motion of the Fermi level relative to the band structure than would be expected from the current results. It must be remembered, however, that the high-field conditions under which the work of Shepherd was carried out causes some broadening of the band. Shepherd, in fact, studied the band broadening as a function of electric field intensity. If his results are extrapolated linearly to zero field, the band width is less than 0.1 eV, a value certainly consistent with the current observations.

We do not know how to interpret in detail the correlations shown by Figs. 2 and 3. They do strongly suggest, however, that the overlayer structure is composition dependent. The optimum structure from the point of view of minimizing the work function is that which maximizes the electron density in the surface states. According to our current model the latter is highest when the magnitude of the loss peak is smallest, i.e. the composition should correspond to region IV of Fig. 3. Since Ericson (ref. 10) has shown that 1 monolayer of Cs is required to optimize the work function, this also implies that the oxygen coverage should be approximately 1/2 monolayer (or less).

It should also be noted that the dipole fields associated with large work function reductions tend to depolarize the individual dipoles. Therefore, other factors being equal, the optimum layer should have the smallest polarizability, i.e. the smallest ϵ . In accord with the ideas in the preceding paragraph, ϵ is found to rise precipitously as we move from region IV into region II, i.e. as the oxygen concentration is increased above 0.5 monolayer.

5. Conclusions

A partially filled band of surface states exists at the valence band edge on the clean Ge(100) surface. This band is responsible for pinning of the Fermi level to the band edge for all conditions of cesium and oxygen coverage. A second surface band occurs approximately 3 eV below the first and excitations between the 2 bands provide an observable feature in the backscattered energy distribution generated by 100 eV primary electrons.

Measurements of the intensity of the 3 eV transition and the bulk and surface plasmon energies lead us to conclude that the overlayer structure is quite composition dependent. The minimum work function configuration appears to correspond to 1 monolayer of Cs and 1/2 monolayer of oxygen and to be such that the surface state band at the valence band edge is completely filled. Furthermore, the structure appears to correspond to a minimum polarizability of the overlayer.

III. STUDIES OF $\text{Na}_2\text{KSb}(\text{Cs})$ PHOTOCATHODES.

At the beginning of these studies it was speculated that application of Auger electron spectroscopy might provide information concerning the formation of $\text{Na}_2\text{KSb}(\text{Cs})$ photocathodes. It appears that some new insight was achieved, and comments about the results from these studies are included in the following paragraphs.

1. The substrate material might not be a significant factor in the control of $\text{Na}_2\text{KSb}(\text{Cs})$ photocathode formation. Although commercial production does not use Ta substrates (as used in these studies), the lack of sample contamination by carbon and oxygen (contaminants of the Ta substrates) may have implication for commercial producers since Carbon and oxygen are highly probable contaminants of many substrate materials.
2. Comments regarding a possible role for oxygen in the formation of $\text{Na}_2\text{KSb}(\text{Cs})$ photocathodes can only be made in a negative sense. In the AES spectrum from the sample with the highest spectral yield found in these studies, there was no peak for oxygen. One can say that oxygen is not required to achieve high photosensitivity.
3. Remarks regarding surface contamination must also be made in a negative sense. Very little contamination of the samples (occasionally oxygen) was encountered. No evidence of contamination was found in the case of the highest spectral yield.
4. There was no exploration of the question regarding photocathode fatigue.
5. Although AES is normally only associated with identification of species in the surface region of a sample it might also provide information concerning bulk composition as was the case in these studies. AES can be used to study alkali antimonide materials, but care must be taken to see that the samples are not changing as a result of the analysis technique.
6. The need for heating the samples to at least 200°C at the $2\text{Na} + \text{K}_3\text{Sb} \rightarrow 2\text{K} + \text{Na}_2\text{KSb}$ stage of formation appears to be related to the need to produce an antimony rich sample, which is related to a cubic crystal structure. "p" type conductivity and high photosensitivity can also be achieved with heating to 175°C (and perhaps $<175^\circ\text{C}$) if excess Sb is deposited during formation.
7. It is possible that the problems with control of the threshold region response of $\text{Na}_2\text{KSb}(\text{Cs})$ photocathodes are associated with the existence of an alkali overlayer. The results of these studies support the idea that there is an alkali overlayer on samples with high photosensitivity. The number, and perhaps species, of overlayer atoms might be subject to sample temperature and crystal structure. (The crystal lattice can affect the binding sites of the overlayer atoms.)

8. The success of an attempt to deposit an alkali specie on a multialkali sample (especially if the substrate is heated) would probably be affected by the same factors that determined which alkali specie left a sample when it was heated (the temperature and the relative populations of the alkali constituents). This might explain some of the inconsistencies found in commercial production. The same deposition procedure may be successful or unsuccessful depending on the consistency of the output of the alkali source, and perhaps the success (or lack of success) of previous alkali deposition attempts. This entire matter could be even more confused if the alkali source outputs are cross-contaminated with other alkali species as was found to be the case in these studies.

9. One important conclusion is general and could easily be overlooked. That conclusion is that Na_2KSb (Cs) photocathodes of high sensitivity can be successfully deposited in a large ultra high vacuum chamber as used here. This had not been achieved previous to these studies. A large experimental chamber allows for the use of many analytical instruments for the study of the films. These remarks lead quite naturally to suggestions for continued investigations. If studies of Na_2KSb (Cs) photocathodes are continued, analytical tools other than AES should be considered. Compared with AES, improved sensitivity to the chemical composition of only the first atomic monolayer could be achieved (ISS), or information regarding the chemical bonding in the samples could be obtained (ESCA). In short, other analytical tools could provide much new information that might be of value in understanding the Na_2KSb (Cs) formation process. The present approach using AES could certainly be continued. In this area a calibration of the AES peak heights for Sb and K or Cs for K_3Sb and Cs_3Sb would be of value in analyzing the AES results from the multialkali samples. More analysis using the relative changes in the Cs AES peaks at 47 and 565 eV could be used to see if Cs is the most significant (or only) constituent of the alkali overlayer on Na_2KSb (Sb) photocathodes of ever higher photosensitivity. Of course samples with a range of high sensitivities would be required for this, and that brings up the final remarks regarding further investigations. No matter which method of sample analysis is chosen, a modification of the sample formation apparatus should be done to allow for continuous monitoring of sample photoemission during constituent depositions. The present deposition and monitoring scheme is too cumbersome, and the success of sample formation too subject to chance.

IV. AN ELECTRICAL, CHEMICAL AND STRUCTURAL STUDY OF THE GE(100)-Cs-O PHOTOCATHODE.

A work function of $.95 \pm .10$ eV and a white light sensitivity of 45 $\mu\text{a/lumen}$ was achieved on an intrinsic Ge(100) sample via the application of cesium and oxygen. The activation procedure was the same as the two-step process used to achieve NEA on Si(100), that of saturating the clean surface with cesium and then maximizing the photoelectric yield with oxygen. While the work function value

is not low enough to be able to achieve NEA on a strongly p-type sample, the photoelectric results indicate that the white light sensitivity would be improved somewhat. Even if it were possible to achieve NEA with germanium, the dark current would undoubtedly be too large for many applications.

The principal value of the present study was the insight added to the semiconductor-Cs-O activation process which at the present time is not well understood. While an exact structural model was not deduced from the experimental results, the evidence was clear that the Levine structural model did not apply to Ge/Cs/O, contrary to expectation. It would be informative to carry out the same investigation with Si/Cs/O, since preliminary results for that system indicate that one-half monolayer of cesium may not be sufficient to achieve NEA. Cesium saturation was found to occur at a coverage beyond the work function minimum, contrary to one of the basic assumptions of the model. A modification might be required allowing a basis of two rather than one cesium atom per site on the 2x1 surface net.

Another important result of the experiment was the observation of surface state emission in the photoemission. The Ge/Cs and Ge/Cs/O EDC's near 3.0 eV photon energy were particularly interesting because the behavior there, previously attributed to bulk emission, was very likely due to transitions involving surface states. The direct behavior of the surface state emission was also interesting. The photoelectric measurements should be extended to higher photon energies and measured with better resolution in order to increase confidence in the observations.

Finally, the usefulness of the ESER (elastic specular electron reflection) technique in structural determination was also demonstrated. It was possible, for example, even without identifying the exact origin of the diffraction peaks, to extract useful information concerning adsorption processes. The curves were also helpful in identifying and comparing surfaces. Because of the wealth of potentially valuable structural information contained in the ESER data, more effort should be expended in the future in the theoretical interpretation.

V. A STUDY OF ELECTRON SCATTERING FROM GE(100).

Low energy electron scattering measurements were conducted as a function of scattering angle and primary energy for an atomically clean Ge(100) sample. These measurements were carried out in an attempt to characterize the different types of electronic processes that occur under low energy bombardment and to assess the role the surface plays in these scattering processes. Although none of the observed effects were found to be peculiar only to Ge, such low energy electron scattering data has not been obtained previously for Ge.

Measurements of the LEED pattern for the clean, annealed surface indicate the probable existence of a Ge(100) 4×2 surface structure. This conclusion is based on the existence of a set of $1/4$ -order diffraction beams that have been in question from previous experiments. Analysis of the LEED beam intensity maxima was accomplished by plotting the incident electron wave vector, corrected for inner potential, on a K-space diagram for the plane of incidence. An inner potential of 14 eV was obtained for primary energies greater than 30 eV. Through such an analysis, most elastic maxima were determined to be Bragg peaks or secondary Bragg peaks due to multiple scattering. This method of analysis showed the potential for easily identifying the diffraction beams that are coupled in the multiple scattering process.

Inelastic electron energy distribution measurements showed the existence of a number of energy loss peaks that are attributed to interband excitations of lattice electrons. These losses were only observed when the sample surface was clean and well ordered. Some of these losses were in fair agreement with band gaps determined by optical measurements and with band structure calculations; however, positive assignment of some electron transitions was not possible. In addition to the interband losses, both surface and bulk plasmon losses and combinations of these losses were observed and their energies were in good agreement with reported values. Future measurements of the inelastic spectra should be made with improved energy resolution for the primary electron beam in order to separate the losses more effectively. In principle it is possible, with better energy and angular resolution, to obtain the E vs. K dependence of the energy bands by careful measurement of the indirect excitations.

Inelastic electron diffraction effects were observed in measurements of both the energy and angular distributions of the inelastic electrons. Results were obtained corresponding to processes where the primary electrons were diffracted before and after energy loss. The qualitative behavior observed in these measurements is in agreement with current theoretical models and for certain instances, where particular Bragg relations could be identified, quantitative evaluations of peak energies and angles were possible. Any additional work done in this area should be carried out on an Al(100) sample to complement the theoretical work being done.

Results of the secondary electron energy distribution measurements indicate the existence of secondary peaks due to two mechanisms. In one, peaks are formed by secondary electrons that satisfy strong diffraction conditions. These peaks were found to correlate very well with the energies and directions of elastic intensity maxima. Variations of the peak energy with scattering angle were calculable in the cases of two peaks where the particular Bragg relations involved could be determined. Over a limited angular range, kinematical Bragg scattering was found to describe the measured peak variation. The second possible mechanism giving rise to secondary peaks is one in which secondary electrons are directly

emitted from regions of local maxima in the conduction band density of states. Correlations were obtained between the energies of secondary peaks measured in the [100] and [111] crystal directions and predicted energies of density of states maxima obtained from band structure calculations. Such measurements show promise as a method for determining the shape of the conduction bands and are worth pursuing in more detail. For both mechanisms a well ordered surface was necessary for observation of structure.

A future experiment that could be done with this apparatus is the measurement of secondary electron energy distributions for surfaces with overlayers, e.g. a cesium overlayer. The accompanying work function lowering would allow the deeper lying conduction bands to be examined. Also, by measuring shifts in the energy band peaks with overlayer coverage, the band bending could be determined directly. This latter measurement has importance in the study of negative electron affinity photocathodes. The advantage this method has over techniques like photoemission, is that where photons penetrate deeply into the solid, low energy electrons penetrate only the first few atom layers; thus, features in the electron scattering measurements reflect energy states near to the surface. In negative affinity photocathodes the space charge region at the surface is often very thin so that electrons, unlike photons, could be effective in measuring changes in the electron states of this region.

VI. PHOTOELECTRIC AND WORK FUNCTION STUDIES OF THE Si(100)-Cs-F SURFACE

A rather complete model for the adsorption behavior of CsF molecules on the Si(100) surface was obtained through the use of Cs and CsF work function vs. coverage and LEED results. The model that is proposed is that the CsF molecule dissociates upon adsorption with, for $\theta < 0.16$, the Cs adsorbing in a 2×1 unit mesh on the pedestal sites and the F adsorbing into the cave sites, possibly in a 2×1 unit mesh. For higher coverages, molecular fields cause the pedestal site to become the energetically favorable site for F adsorption, especially for $\theta > 0.23$. The adsorption of F onto the pedestal sites prevents the ordered adsorption of Cs onto the pedestal sites (large background in the LEED pattern) and also causes some Cs to adsorb into the valley sites. At $\theta = 0.45$, most of the available bonding sites are occupied so that the sticking coefficient decreases substantially for higher coverages.

The Cs and CsF dipole moments and polarizabilities on Si(100) were determined experimentally from the work function vs. coverage results through the use of a work function reduction model that takes into account depolarizing effects.

Of prominent interest was whether Cs and CsF could be adsorbed in certain amounts and orders to yield a work function low enough

for NEA on Si (1.1 eV). The resulting work function values for the various deposition procedures are listed in the following table:

Deposition Procedure	Work Function (eV)
Cs (1/2 monolayer)	1.05
Cs (1 monolayer)	1.45
CsF (1/4-1/2 monolayer)	1.85
CsF (1/2 monolayer)-Cs	1.40
Cs (1 monolayer)-CsF	1.05
Cs (1/2 monolayer)-CsF	0.80
Cs (1 monolayer)-O	0.75

Depositing 1/2 monolayer of Cs and then CsF and also depositing one monolayer of Cs followed by O, gave the optimum work function reductions. The final Cs coverage on both low work function surfaces was one monolayer of Cs rather than the 1/2 monolayer proposed by Levine.

The photoyield results indicate that the work function value (measured with the Farnsworth gun) can be low enough for NEA, and yet, the resulting photoyield can be quite poor. The reason for the poor photoyield from the low work function surfaces in this experiment is not known but seems to be related in some manner to the density of surface imperfection on the sample. The proper pre-vacuum cleaning, sputtering, and annealing procedures appear to be quite important for the attainment of a good NEA photoyield surface.

A rather interesting result of this experiment was the low threshold and large cross section observed for electron-stimulated desorption of F. Also noted was that there appears to be either a large difference in the desorption cross section or migration rate of F on the CsF surface depending on the order of depositing CsF molecules and Cs atoms.

Several additional experiments appear to be of interest from the results of this experiment. It was observed that the work function obtained from the Si(100)-Cs/F surface (0.8eV) was below that necessary for NEA. Once a sample preparation procedure has been obtained that yields good NEA photoyield from the Si(100)-Cs/O surface, it would be of interest to continue experiments with CsF depositions to determine whether a NEA photoyield can be obtained with CsF.

A low work function value (1.05 eV) obtained by depositing 1/2 monolayer of Cs is very close to the work function value necessary for NEA on Si. One possible method to increase the work function reduction would be to cool the sample to liquid-N₂ temperatures to increase the band bending. Cooling the sample would have the additional effect of reducing the high dark current observed for Si(100) NEA photocathodes.

The SEM photomicrographs and the results of the Si chemical cleaning experiments indicate that there is much that is not known about the proper cleaning procedure for the Si(100) surface. An experiment studying the defect structures created by high temperature heating in a vacuum or defect structures created by sputtering would be useful. An experiment using AES to study the chemical composition of thin surface films produced by the various chemical cleaning procedures would have vast technological importance to the semiconductor industry where such cleaning procedures are frequently used.

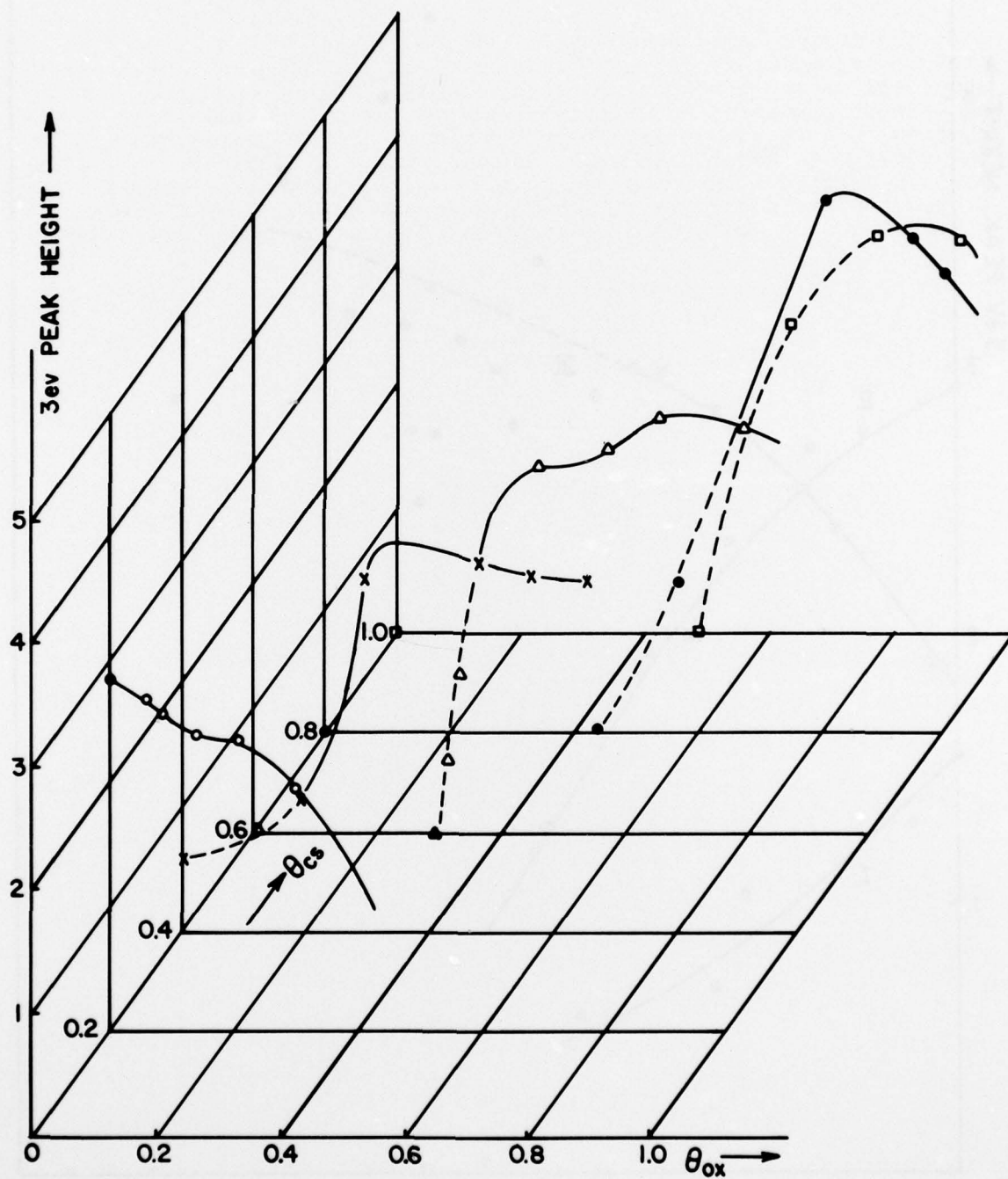


FIGURE 1 Magnitude of the 3eV electron energy loss of Ge(100) vs. chemical composition of the Cs-O overlayer.

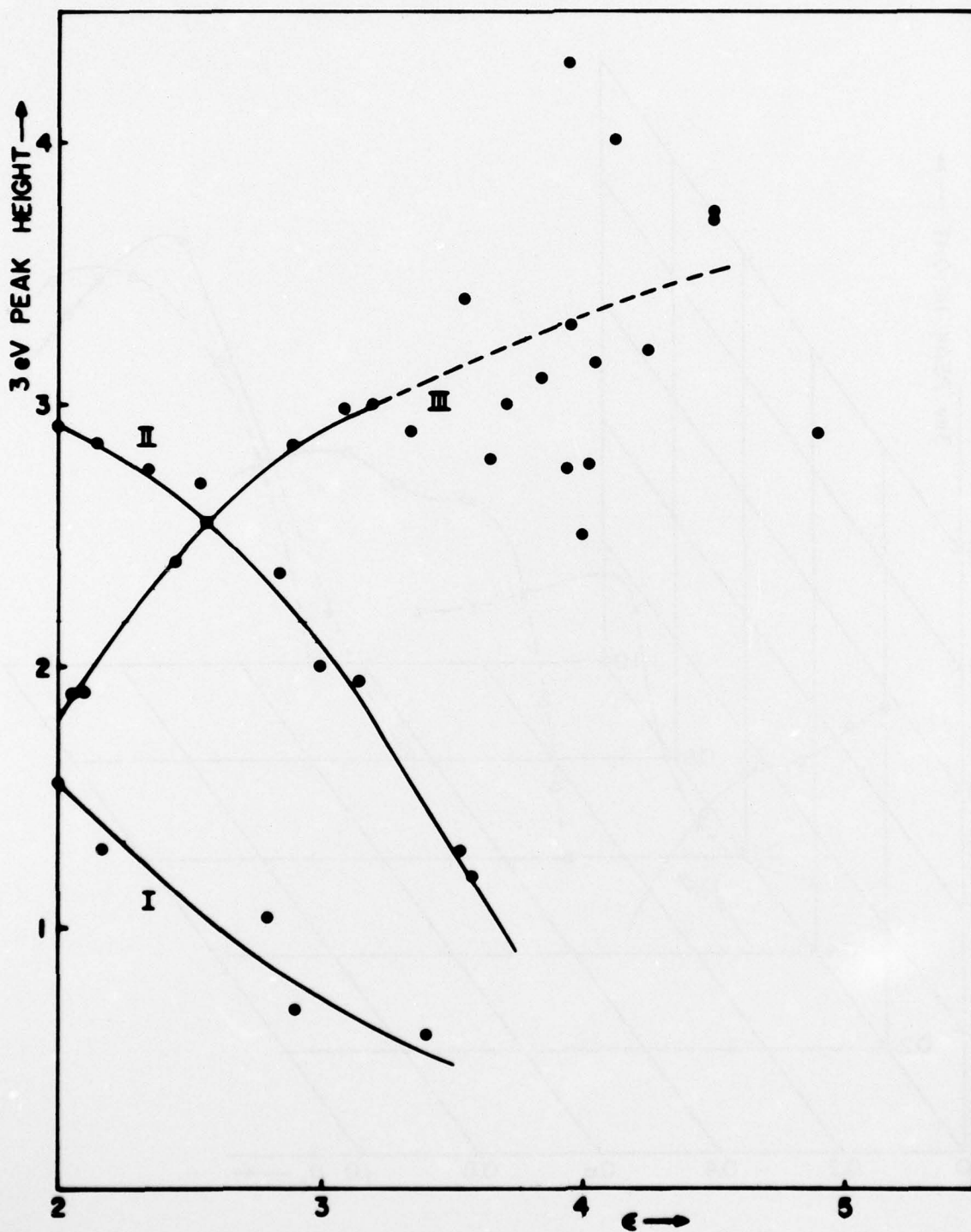


FIGURE 2 Magnitude of the 3eV electron energy loss on Ge(100) vs. the effective dielectric constant of the overlayer.

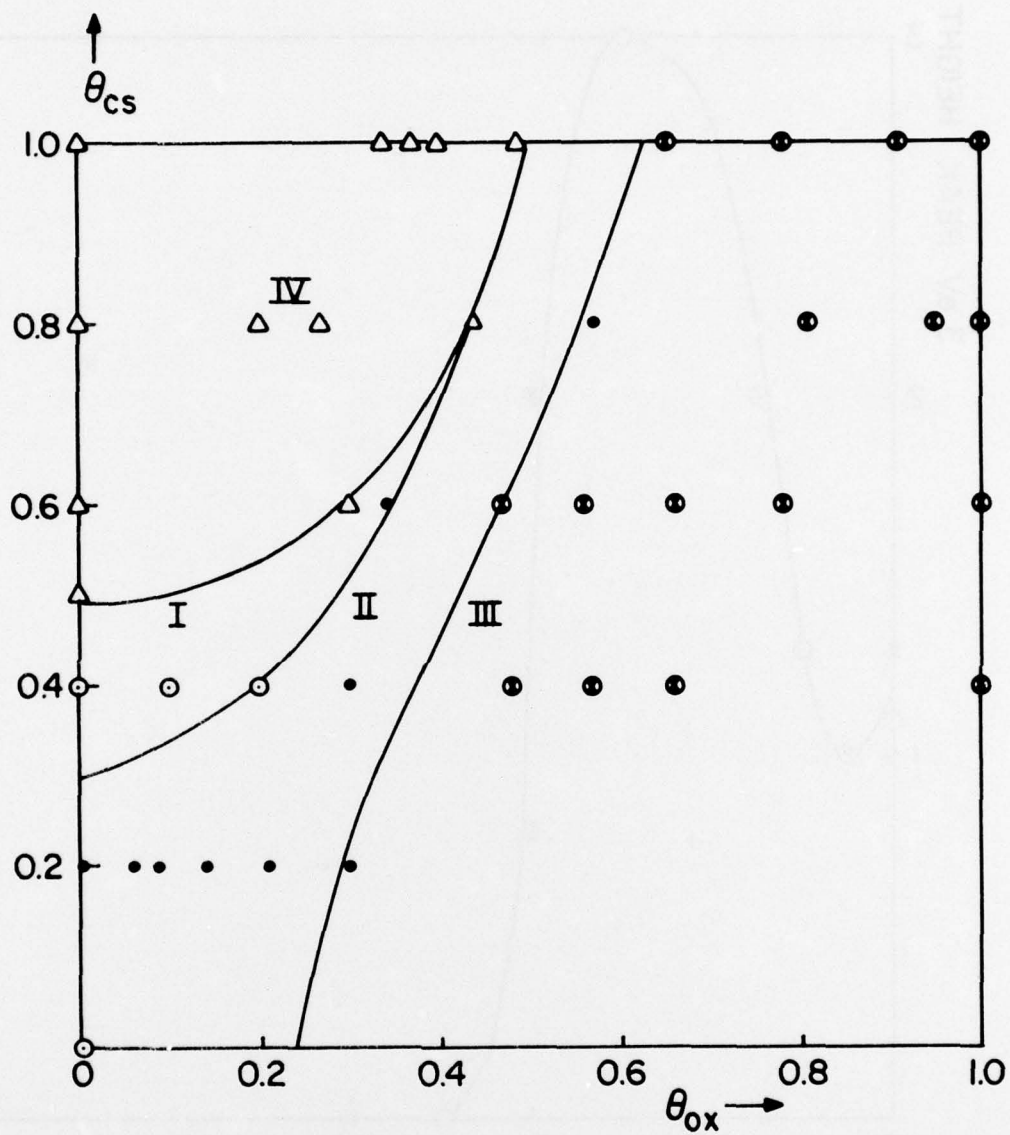


FIGURE 3 Phase diagram showing the composition ranges in which the various branches of Fig. 2 are valid.

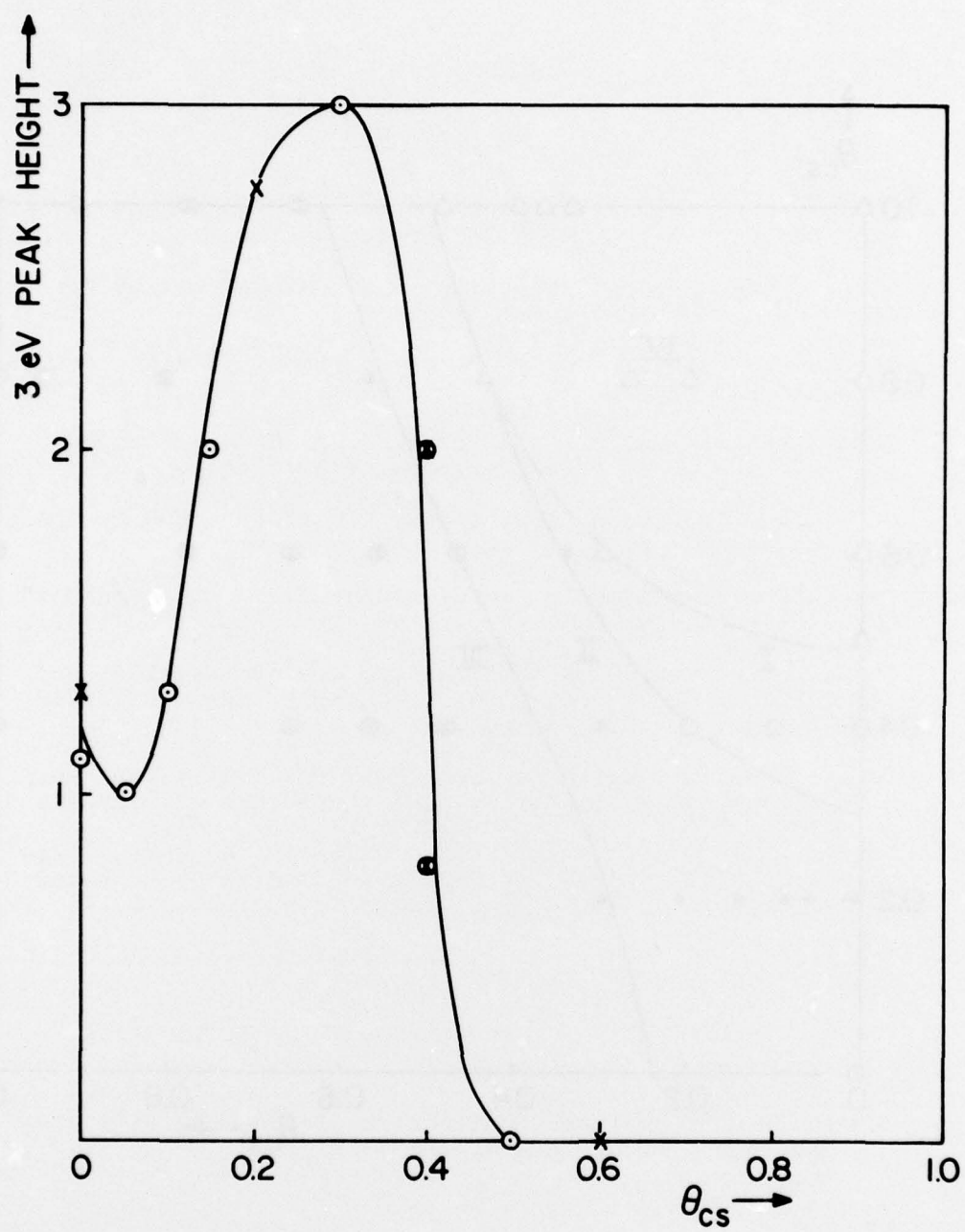


FIGURE 4 Magnitude of the 3eV electron energy loss on Ge(100) vs. Cs coverage.

LIST OF REFERENCES

1. Proposal (September 11, 1968) in response to RFQ No. DAA KO2-69-Q-0027 from Fort Belvoir, Va., p. 2.
2. "A Study of Electron Scattering from Germanium (100)", R. L. Erickson, AFAL-TR-76-36.
3. "Research in Physics of Electron Emission and Electron Tube Technology", AFAL-TR-66-250, volume III, p. 25.
4. "Aluminosiliate Alkali Ion Sources", R. E. Weber and L. F. Cordes, Rev. Sci. Instr. 37, 112 (1966).
5. "Physics of Electron-Electron and Electron-Photon Interaction", AFAL-TR-69-177, p. 58.
6. "Surface Plasma Oscillation of a Degenerate Electron Gas", E. A. Stern and R. A. Ferrel, Phys. Rev. 120, 130 (1960).
7. "A Photoelectron Study of Clean and Cesiumated Si(100) and Ge(100)", M. R. Jeanes and W. M. Mularie, AFAL-TR-72-242, p. 120.
8. "Photoemission Studies of the Alkali-covered Ge(100) Surface", G. E. Riach and W. T. Peria, Surface Science 40, 479 (1973).
9. "Observation of Surface-State Emission in the Energy Distribution of Electrons Field-Emitted from (100) Oriented Ge", W. B. Shepherd and W. T. Peria, Surface Science 38, 461 (1973).
10. "An Electrical Chemical and Structural Study of the Ge(100)-Cs-O Surface", R. E. Ericson AFAL-TR-76-34.
11. "Studies of Na₂KSb(Cs) Photocathodes", P. A. Lindfors, AFAL-TR-76-38 .
12. "Photoelectric and Work Function Studies of the Si(100)-Cs/F Surface", F. J. Kub, AFAL-TR-76-37.